Truncated form of human CD19 antigen as a suicide gene to control T-cell alloreactivity: *ΔCD19*

Simona Manni,[1] Laura Iaffaldano,[1] Marika Guercio,[1] Pietro Merli,[1] Francesca Del Bufalo,[1] Marco Becilli,[1] Mattia Algeri,[1] Daria Pagliara,[1] Rita De Vito,[2] Gerhard Zugmaier,[3] Biagio De Angelis,[1] Concetta Quintarelli[1,4#] and Franco Locatelli[1,5#]

[1]Department of Onco-Hematology and Cell and Gene Therapy, Bambino Gesù Children's Hospital, IRCCS, Rome, Italy; [2]Pathology Unit, Department of Laboratories, Bambino Gesù Children's Hospital, IRCCS, Rome, Italy; [3]Amgen Research (Munich) GmbH, Munich, Germany; [4]Department of Clinical Medicine and Surgery, Federico II University of Naples, Naples, Italy and [5]Department of Life Sciences and Public Health, Catholic University of the Sacred Heart, Rome, Italy

[#]*CQ and FL contributed equally as senior authors.*

Correspondence: F. Locatelli
franco.locatelli@opbg.net

B. De Angelis
biagio.deangelis@opbg.net

Received: January 13, 2025.
Accepted: April 23, 2025.
Early view: April 30, 2025.

https://doi.org/10.3324/haematol.2025.287364

Abstract

Donor lymphocyte infusion (DLI) is employed to either treat or prevent relapse in patients with hematologic malignancies, as well as to accelerate recovery of adaptive immunity, after allogeneic hematopoietic stem cell transplantation (allo-HSCT). With the increased use of DLI, there is renewed interest in the development of approaches able to prevent graft-*versus*-host disease (GVHD). In this study, we describe a novel and effective safety switch represented by the truncated form of the human CD19 antigen (ΔCD19) used to transduce T lymphocytes (hΔCD19 T cells). We demonstrated that the exposure of ΔCD19 T cells to an anti-hCD19-hCD3 T cell bi-specific T-cell engager (BiTE) molecule (structurally identical to blinatumomab, an agent largely used in the treatment of B-cell acute lymphoblastic leukemia) resulted into a prompt elimination of hCD19$^+$/CD3$^+$ cells both *in vitro* and in an *in vivo* animal model of mice developing a xenograft reaction mimicking GVHD after infusion of *in vitro*-activated/expanded human T cells. Importantly, the administration of the anti-hCD19-hCD3 BiTE molecule in the animal model, on one hand led to the improvement of signs and symptoms of GVHD, as well as of the overall-survival of the mice, and on the other hand, after a drug washout, was associated with the resurge of ΔCD19 T cells without re-occurrence of GVHD. Our study provides evidence that the *ΔCD19* suicide gene used in combination with an anti-hCD19-hCD3 T-cell BiTE molecule could represent a valid and effective strategy to control GVHD occurring after the infusion of donor T lymphocytes.

Introduction

Allogeneic hematopoietic stem cell transplantation (allo-HSCT) is largely used to treat patients affected by several malignant and non-malignant disorders.[1,2] In patients with hematological malignancies, the therapeutic effect of allo-HSCT mainly lies on the immunological capability of donor T lymphocytes to activate graft-*versus*-leukemia (GVL) effect.[3,4] Donor lymphocyte infusions (DLI) are a critical therapeutic strategy used to leverage GVL, particularly for patients who experience relapse after HSCT.[5] Current research efforts aim to enhance DLI efficacy and safety, also including the use of *ex vivo*–stimulated donor T cells.[6] GVL is largely associated with the graft-*versus*-host disease (GVHD) phenomenon, where donor immune cells attack not only tumor cells, but also recipient healthy tissues.[7,8] With an incidence ranging from 40% in matched related donor (MRD) transplants to 70% in matched unrelated donor (MUD) transplants for grade 2-4 acute GVHD, or from 30% to 70% for chronic GVHD following allo-HSCT,[9,10] GVHD requires careful consideration, as it is associated with morbidity and mortality that significantly limit the curative potential of allo-HSCT and DLI. Nevertheless, in the context of hematologic malignancies, a close correlation between leukemia eradication and development of GVHD has been demonstrated,[11] expecially after the use of DLI.[12]

Approaches of donor T-cell depletion based on either the positive selection of CD34$^+$ hematopoietic stem cells (HSC) or broad negative selection of T lymphocytes, have been developed with the goal of reducing GVHD incidence and severity especially when the donor shows HLA disparities with the recipient.[13] However, these approaches are not

without limitations. Indeed, the transplant with positive selection of CD34$^+$ HSC implies the loss of all immune subsets able to protect the patient against infections, to eliminate residual leukemia cells and to support the sustained engraftment of donor cells,[14] while the depletion of CD3$^+$ T cells jeopardizes both the protection against pathogens conferred by antigen-experienced T lymphocytes transferred with the graft and the T-cell mediated GVL effect.[15] In light of these considerations, refinements of graft manipulation approaches have been developed, including the selective depletion of TCR$\alpha\beta^+$ lymphocytes, which allows to preserve in the graft not only natural killer cells, monocytes and dendritic cells, but also $\gamma\delta$ T lymphocytes.[16,17] Although selective TCR$\alpha\beta^+$ T-cell depletion has shown remarkable efficacy in children with acute leukemia,[18,19] there is still the usolved problem of a delayed recovery of adaptive immunity conferred by TCR$\alpha\beta^+$ lymphocytes in comparison to patients receiving an unmanipulated graft.[20] In order to accelerate the post-transplant recovery of adaptive TCR$\alpha\beta^+$ T-cell immunity, a promising approach is that based on the use of DLI. Indeed, beyond treating relapse after HSCT, DLI are now used in recipients of T cell-depleted grafts to fasten immune recovery. In this scenario, novel strategies have been developed to improve the efficacy and safety profile of unmanipulated DLI, including *ex vivo*-activated donor-derived T cells,[6] and donor T cells genetically modified with a suicide gene to reduce or modulate the occurence of GVHD. Specifically, the inducible caspase-9 (*iC9*) suicide gene is one activable safety switch that has been used to genetically modify donor T cells with the goal of controlling side effects related to DLI. In case of GVHD occurence, the AP1903 dimerizing drug activating iC9 is administered, resulting in the elimination of 85-95% of circulating CD3$^+$ T cells within 30 minutes, with no recurrence of GVHD in the majority of treated patients.[21-23] Unfortunately, currently, the dimerizing agent AP1903 is not commercially available, making it inaccessible for treatment of patients outside specific trials.

We developed a pre-clinical, innovative strategy based on the use of ΔCD19, a new suicide gene represented by the CD19 truncated form, which can be targeted using an anti-hCD19-hCD3 T-cell bi-specific T-cell engager (BiTE) molecule, which is structurally identical to blinatumomab, a commercially available drug approved for the treatment of adult and pediatric patients with B-cell precursor ALL.[24-26] Using *in vitro* and *in vivo* preclinical models, we proved that this system allows a prompt elimination of the most alloreactive ΔCD19 T cells, preserving the survival of non-activated/non-alloreactive T cells which, after drug discontinuation, are able to re-expand without subsequent GVHD occurrence.

Methods

ΔCD19 T-cell generation

Human polyclonal T cells were activated and transduced, as previously described,[27] with a retroviral vector encoding the codon-optimized sequence of the ΔCD19 antigen (extracellular region in-frame with the transmembrane region of human CD19, NCBI-GenBank: AH005421.2).

Suicide gene functional assays

For *in vitro* assays, hΔCD19 T cells were treated twice a day for 3 days with 10, 50, 100 ng/mL of anti-βGal-hCD19 (InvivoGen, France, Cat. BIMAB-HCD19BGAL) or anti-hCD19-CD3 (InvivoGen, France, Cat. BIMAB-HCD19CD3).

For *in vivo* assays, Cg-Prkdcscid Il2rgtm1Wjl/SzJ (NSG) female mice were provided by Charles River. All animal procedures were performed in accordance with the Guidelines for Animal Care and Use of the National Institute of Health (Prot. No. 088/2016-PR). Mice were intravenously (i.v.) infused with 20x10^6 T cells enriched for the expression of hΔCD19 by anti-CD19 microbeads (Miltenyi, USA), with the purity of 98.5%. Mice also received intra-peritoneally (i.p.) 1,000 IU recombinant human interleukin 2 (Il2) (hIL2, R&D, USA) twice a week. As negative control of GVHD, four mice were injected with only hIL-2 twice a week. At time of the xeno-GVHD occurrence, mice infused with hΔCD19 T cells were randomized in two cohorts, receiving either anti-βGal-hCD19 control (1 ug/mice/day) or anti-hCD19-CD3 (1 ug/mice/day) by i.v. injection for two drug administration cycles of 5 days each.

Phenotypic analysis

Flow-cytometry analysis was performed using anti-human CD45, CD3, CD4, CD8, CD62L, CD45RA, CD19 antibodies (BD Biosciences, USA). Flow-cytometry analysis was performed using a BD LSRFortessa X-20 cytometer (BD Biosciences, USA) and analyzed by FACSDiva software (BD Biosciences, USA).

Graft-*versus*-host disease score

Mice were evaluated daily for the occurrence and severity grading of GVHD. In particular, the following score was assessed by blinded operators of experimental procedures on animals: GVHD score 0 (no sign of GVHD); GVHD score 1 (mice with loss and/or ruffled fur; no additional suffering); GVHD score 2 (mice developing over 10% of weight loss and fur loss; no additional suffering); GVHD score 3 (mice showing over 10% of weight loss and complete fur loss and/or ocular alterations and/or low motility).

Histopathologic analysis

The histopathologic analysis was performed as previously reported,[28,29] using anti-CD3 antibody (1:100, DAKO) as primary antibody and secondary biotinylated antibody (K8024, Dako, Carpinteria, USA). Analysis was performed using Zeiss microscope. The immunofluorescence analysis was performed using anti-CD3 antibody (1:100, DAKO) or anti-Ki67 antibody (1:100, Abcam) as primary antibodies and Alexa Fluor 488 and Alexa Fluor 455 (Invitrogen, Carlsbad,

CA, USA) as secondary antibodies, respectively. Cells were counterstained with DAPI and analysis was performed using the Olympus microscope FV3000. Immunohistochemistry and immunofluorescence images have been collected through ScanScope XT scanner and digitized to scalable images by NDPVIEW V.2 software.

Cytokine analysis

Human IFNγ, IL-2, TNF-α, IL-10 were analyzed by ELLA automated enzyme immunoassay system (Bio-Techne, CA, USA) using Simple Plex software.

Statistical analysis

Data are expressed as mean ± standard deviation (SD). Student *t* test (two-sided) and Pearson correlation coefficient (r) were used to determine statistically significant differences between samples, with *P* value <0.05 indicating a significant difference. Survival data were evaluated using Kaplan-Meier survival curves and the Fisher's exact test was used to measure differences between animal cohorts. The IF/IHC image data were quantified using ImageJ software. Graphic representations and statistical analysis were performed using GraphPad Prism 6.

Results

Engineered ΔCD19 T cells are targeted and *in vitro* eliminated by anti-hCD19-hCD3 bi-specific T-cell engager

To obtain preliminary evidence of the functionality of the *ΔCD19* suicide gene, whose mechanism is described in Figure 1A, peripheral blood mononuclear cells (PBMC) derived from HD were genetically modified to obtain expression of the ΔCD19 molecule by transduction with the construct shown in Figure 1B. First, we sought to evaluate if ΔCD19 expression induced any change in terms of proliferation and cell population distribution profile compared to control non-transduced (NT) T cells. We observed that the high expression of the *ΔCD19* suicide gene in genetically modified T cells (hΔCD19 T cells) (Figure 1C) did not induce any change, in terms of fold expansion (Figure 1D) and in $CD4^+/CD8^+$ distribution (Figure 1E) as compared to control NT T cells.

Thereafter, we tested the ability of the anti-hCD19-hCD3 BiTE (an antibody featuring blinatumomab's single-chain variable fragments [scFv] joined by a glycine-serine linker and a hexahistidine tag [His6]) to target and kill hΔCD19 T cells in culture assays at pre-defined time points. For this purpose, culture assays were performed in the presence of either the bi-specific anti-hCD19-hCD3 or the anti-βGal-hCD19 (used as a negative control and characterized by a scFv specific for human CD19 joined by a glycine-serine linker and a His6 to the scFv of an antibody binding *E. coli* β-galactosidase). The concentration of anti-hCD19-hCD3 or anti-βGal-hCD19 was comprised in the range of 10-100 ng/mL. We observed a complete elimination from the culture of hΔCD19 T cells already using the lowest concentration of anti-hCD19-hCD3 (10 ng/mL) (Figure 1F shows the data at the 72-hour time point, whereas *Online Supplementary Figure S1A, B* show data at 24 hours and *Online Supplementary Figure S1C, D* at 48 hours, respectively). Nevertheless, a direct correlation was observed between the concentration of anti-hCD19-hCD3 used and the ability to eliminate hΔCD19 T cells from the culture at earlier time points (*Online Supplementary Figure S1B, D)*.

Establishment of an *in vivo* model for xenograft-*versus*-host disease induced by human donor lymphocyte infusions

In order to reproduce a simplified *in vivo* model of GVHD after injection of *in vitro*-activated human T cells, NSG mice received selected hΔCD19 T cells ($20x10^6$/mouse T cells that were 98.5% positive for hΔCD19) generated from a HD and infused by i.v. injection, coupled with biweekly i.p. injections of hIL-2 (Figure 2A). By monitoring mice with weekly bleeding, we observed a significant increase of human $CD45^+CD3^+$ cells by day +56 (Figure 2B) associated with the development of a xenograft reaction mimicking human GVHD sign. Notably, the percentage of circulating $hCD45^+$ cells strongly correlated with weight loss (Figure 2C). Specifically, at this time point, we assessed the GVHD grading observed in the animals according to the score criteria illustrated in Figure 2D. Among the 16 mice infused with hΔCD19 T cells, 25% (4 mice) presented GVHD grade 0 (excluded from further investigations since GVHD was not developed), 18.75% (3 mice) presented GVHD grade 1 and 56.25% (9 mice) presented GVHD grade 2, with a significant weight and fur loss, combined with general low motility (Figure 2E). As a negative control of GVHD, four mice were injected with only hIL-2 twice a week; as expected, these animals did not develop signs of suffering, weight and fur loss (GVHD grade 0) (Figure 2E). Interestingly, we observed a significant correlation between the GVHD score and the level of IFNγ (Figure 2F) and TNF-α (Figure 2G) at day 56.

Anti-hCD19-CD3 bi-specific T-cell engager displays a therapeutic effect in mice developing graft-*versus*-host disease

The ability of anti-hCD19-hCD3 to control GVHD was assessed in the *in vivo* model using the experimental design detailed in Figure 3A. In particular, at day 56, when the majority of the mice infused with hΔCD19 T cells had presented at least grade 1 GVHD, mice were randomized in two cohorts: one given the anti-βGal-hCD19 (1 μg/mice/day, as negative control) and the other one receiving the anti-hCD19-hCD3 BiTE (1 μg/mice/day) for two cycles of 5-day treatment each. Mice not developing signs of GvHD (N=4) were excluded from the experiment.

First, we sought to evaluate whether the interaction be-

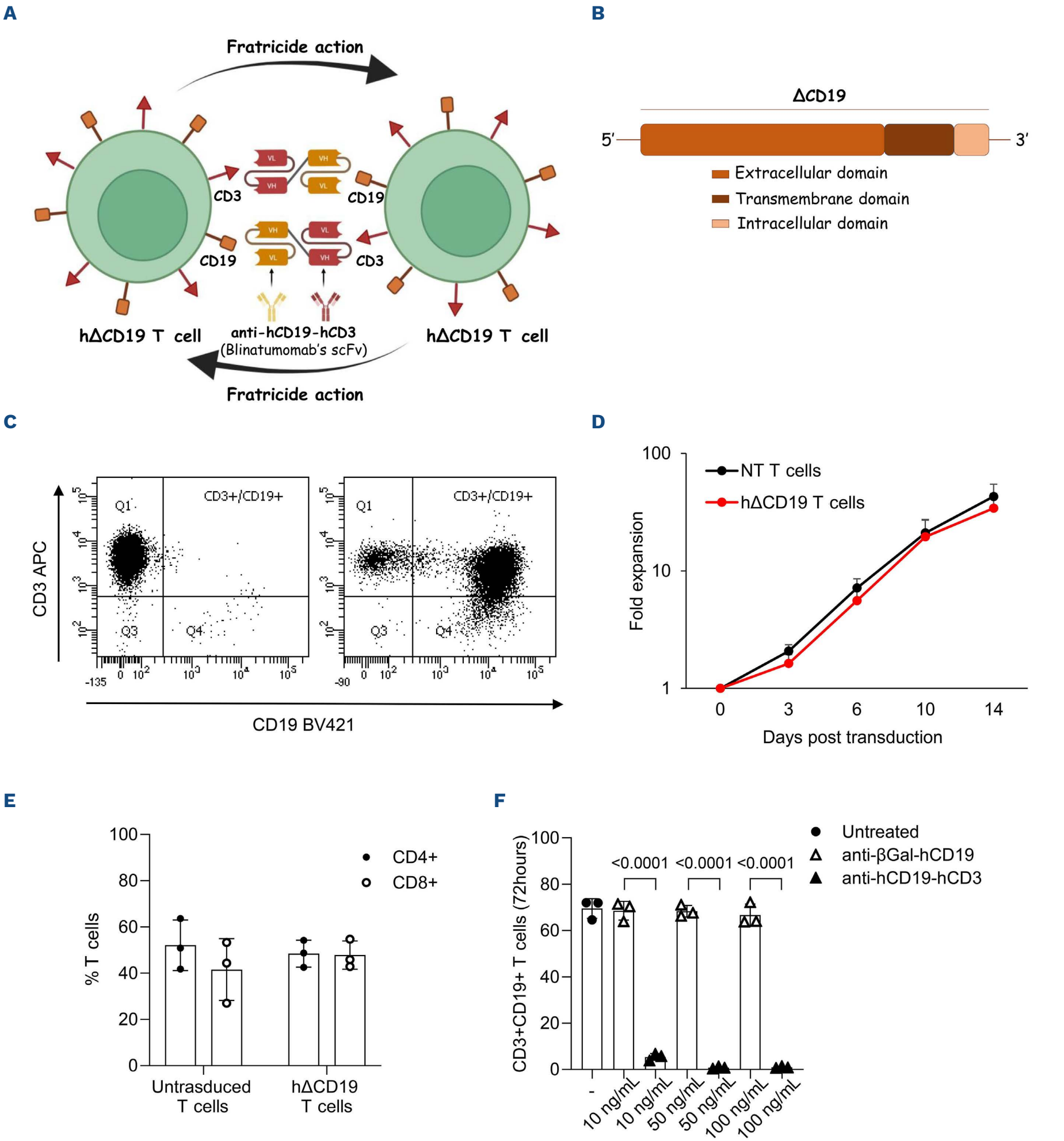

Figure 1. Characterization of hΔCD19 T cells and anti-hCD19-hCD3 *in vitro* activity. (A) The diagram shows the fratricide action of $CD3^+$ T cells transduced with the SFG retroviral construct including the codon optimized *hΔCD19* sequence ($CD3^+CD19^+$) following exposure to anti-hCD19-hCD3 T cell bi-specific T-cell engager (BiTE). (B) Design of the retroviral vector including the *hΔCD19* sequence. (C) Representative flow-cytometry analysis of non-transduced (NT) T cells (left panel) and hΔCD19 (right panel) T cells derived from healthy donors (HD) 5 days after transduction. (D) Fold expansion of NT (black line) and hΔCD19 T cells (red line) in the presence of interleukin 7 (IL7) and IL15. Data from 6 HD are expressed as average ± standard deviation (SD). (E) Fluorescence-activated cell sorting analysis was performed to evaluate the $CD4^+$ and $CD8^+$ cell distribution in NT and hΔCD19 T cells. Data from 3 HD are expressed as individual values ± SD. (F) hΔCD19 T cells were plated at $0.5x10^6$ cells/cm^2 in presence of either the anti-βGal-hCD19 or the anti-hCD19-hCD3 antibodies within the concentration range of 10-100 ng/mL. Drugs were administered twice a day for 3 days. Data from 3 HD are expressed as individual values ± SD.

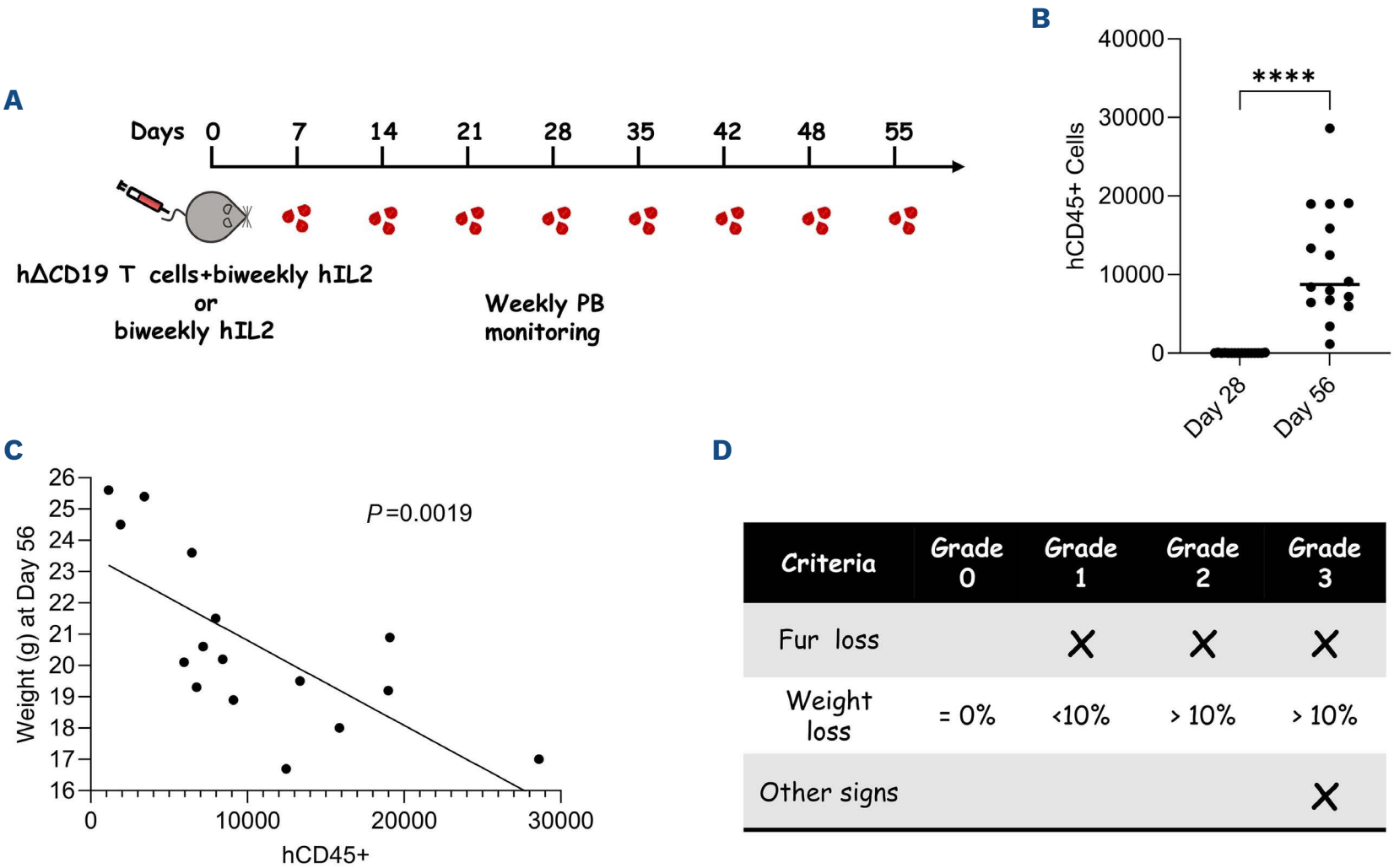

Criteria	Grade 0	Grade 1	Grade 2	Grade 3
Fur loss		X	X	X
Weight loss	= 0%	<10%	> 10%	> 10%
Other signs				X

Figure 2. Characterization of an *in vivo* animal model mimicking graft-*versus*-host disease after engraftment of *ex vivo*-expanded gene modified donor lymphocyte infusion. (A) Schematic representation of the *in vivo* experimental design: mice (N=16) were infused with 20x10^6 hΔCD19 T cells cells/mouse intravenously (i.v.) on day 0 and interleukin 2 h (hIL2) intraperineally (i.p) (1,000 IU) on a twice-weekly basis. Additional mice (N=4) were treated with only human Il2 twice a week as control. The development of skin and ocular graft-*versus*-host disease (GVHD) manifestations was monitored daily, while weight measurements and blood bleeding analysis were performed on a weekly basis. (B) Assessment of the hCD45$^+$ CD3$^+$ cell population in mice before (day +26) and at the onset of GVHD (day +56) was performed by fluorescence-activated cell sorting analysis. (C) Correlation between the percentage of circulating hCD45$^+$ cells and weight at day +56. Pearson correlation coefficient (r) was employed to calculate the strength and direction of the linear relationship between the two continuous variables, and a *P* value <0.05 was considered to be statistically significant. (D) Schematic representation of the score criteria to assess GVHD grading: GVHD grade 0 (no sign of GVHD); GVHD grade 1 (mice with loss and/or ruffled fur; no additional suffering); GVHD grade 2 (mice developing over 10% of weight loss and fur loss; no additional suffering); GVHD grade 3 (mice developing more than 10% of weight loss and complete fur loss and/or ocular alterations and/or low motility). (E) Pie charts showing the GVHD grade developed in all animals undergoing treatment on day 56. IFNγ (F) and TNFα (G) cytokine levels measured on day 56 in the animals undergoing treatment. Data are expressed as individual values. Data from 8 mice are presented instead of 9 for mice developing grade 2 GVHD, as one sample was excluded from the analysis due to a technical issue occurred with the plasma sample. The Student's *t* test was employed to calculate statistically significant differences between groups and a *P* value <0.05 was considered to be statistically significant.

tween the hCD3 scFv of blinatumomab and the hCD3 molecule expressed on T cells could worsen the conditions of mice by triggering T-cell activation. For this purpose, focusing on the evaluation of IFNγ secreted by activated T cells and mediating toxicity,[30] we monitored IFNγ levels in mice peripheral blood at early (3 days after the last BiTE administration) and late (10 days after the last BiTE administration) time points following the first and second BiTE cycle. As shown in Figure 3B, the administration of the initial cycle of anti-hCD19-hCD3 (56-60 days) correlated with a statistically significant decrease in IFNγ levels at day 63 as compared to the control group of mice, which received the anti-βGal-hCD19 drug (Figure 3B, left panel). Since T cells tended to re-expand after treatment discontinuation, at day 70, we also documented that, instead, the IFNγ level did not. Upon re-exposing the mice to the treatment, we observed a further reduction in IFNγ levels not only 3 days post the treatment cycle, but also 10 days later. TNFα level were also significantly reduced after the second cycle of BiTE (Figure 3B, right panel). By contrast, no significant difference was observed for both IL2 (*Online Supplementary Figure S2A*) and IL10 (*Online Supplementary Figure S2B*) levels between the anti-βGal-hCD19 and anti-hCD19-hCD3-treated cohorts at any of the analyzed time points.

Furthermore, in our GVHD murine model, anti-hCD19-hCD3-treated mice demonstrated a significant improvement of the GVHD signs. Specifically, mice treated with the anti-hCD19-hCD3 exhibited a significant weight recovery compared to those treated with anti-βGal-hCD19, reaching levels similar to those of the control animals not developing GVHD (Figure 3C). Figure 3D illustrates exemplificative mice of each cohort, indicating that animals receiving anti-hCD3-hCD19 not only halted fur loss, but also animals did not experience abnormal eyeball growth, in contrast to mice treated with anti-βGal-hCD19. As shown in Figure 3E, the comprehensive evaluation of GVHD manifestations reveals a change in the GVHD severity grading assigned at day 56 (pretreatment) over the course of the experiment.

Specifically, among the animals treated with the anti-hCD19-hCD3 BiTE, four of six mice displayed symptom improvement, including reduced fur loss, weight gain, and a transition from grade 2 to grade 1 (grade 1 considering a not complete fur recovery, in the absence of other signs of GVHD). The remaining two animals treated with the anti-hCD19-hCD3 BiTE, one maintained a GVHD grade 2 without weight recovery, and the other worsening to grade 3 with ocular aberrations. These two non-responder mice showed the most severe GVHD manifestations at day 56 compared to the other animals, having the lowest body weight recorded at time of the first cycle of anti-hCD19-hCD3 BiTE. Of the six animals in the control cohort treated with the anti-βGal-hCD19 control, although IFNγ levels tended to decrease (Figure 2B), two mice failed to regain weight and experienced complete fur loss, maintaining a classification of grade 2 GVHD. The remaining four mice worsened to grade 3 GVHD, exhibiting further signs of the disease, notably abnormal growth of the eyeball (Figure 3E).

Finally, the administration of the anti-hCD19-hCD3 BiTE was associated with better overall survival (OS; Figure 3F), with four of six mice surviving the termination of the experiment, as compared to none of the mice (0/6) in the cohort receiving the control anti-βGal-hCD3 treatment.

Characterization of hΔCD19 T cells resurging *in vivo* after anti-hCD19-CD3 bi-specific T-cell engager treatment

Alongside the evaluation of GVHD signs and the ability of the anti-hCD19-hCD3 to improve the outcome of the treated mice, we sought to study the mechanisms associated with the control of GVHD at the tissue/cellular level.

Figure 4A illustrates the temporal dynamics of hCD45$^+$ cells over the course of the experiment in the two cohorts: one treated with the anti-hCD19-hCD3 (top panel) and the other treated with the control anti-βGal-hCD19 (bottom panel). By day 56, we observed a significant expansion of hCD45$^+$ cells in the experimental mice, which coincides with the onset of toxicities, such as fur loss and weight loss. This time point marks the start of the treatment cycles, as indicated by the arrows in Figure 4A, B (day +56 for the first cycle and day +70 for the second cycle). By day 63 (namely 3 days after the conclusion of the first anti-hCD19-hCD3 treatment cycle of 5 consecutive days), a statistically significant decrease in the absolute number of hCD45$^+$ cells were observed in the cohort treated with anti-hCD19-hCD3 (Figure 4A, top panel), in contrast to the cohort treated with the control anti-βGal-hCD19 (Figure 4A, bottom panel), which did not show a similar decrease. Notably, in the anti-hCD19-hCD3-treated cohort, hCD45$^+$ cell levels significantly decreased for further 3 days after the conclusion of the second treatment cycle (Figure 4A, top panel). CD19-positive T cells, which represent nearly the whole hCD45$^+$ population infused (98.5% of purity) into the mice, were significantly reduced very early after discontinuation of the first anti-hCD19-CD3 cycle (day 63) (Figure 4B, upper panel), in contrast to the cohort treated with the control anti-βGal-hCD19 (Figure 4B, bottom panel), which did not show a similar decrease. Then, we observed a tendency (although not statistically significant) of hCD3$^+$CD19$^+$ population to re-expand after 3 days from the end of the first BiTE cycle (day 70). In particular, the absolute number of hCD3$^+$ CD19$^+$ cells detected at day 70 was significantly lower than that at day 56 in the same mouse cohort (Figure 4B, upper panel) and decreased further after the second round of anti-hCD19-hCD3 treatment, confirming that persisting hΔCD19 T cells were still responsive to the anti-hCD19-CD3 BiTE (Figure 4A, B, upper panels). In addition, no modulation of the absolute number of CD19-negative hT cells, whose levels in terms of absolute numbers are negligible with respect to CD19$^+$ T cells, was observed in both the anti-hCD19-hCD3-treated cohort (Figure 4C, upper

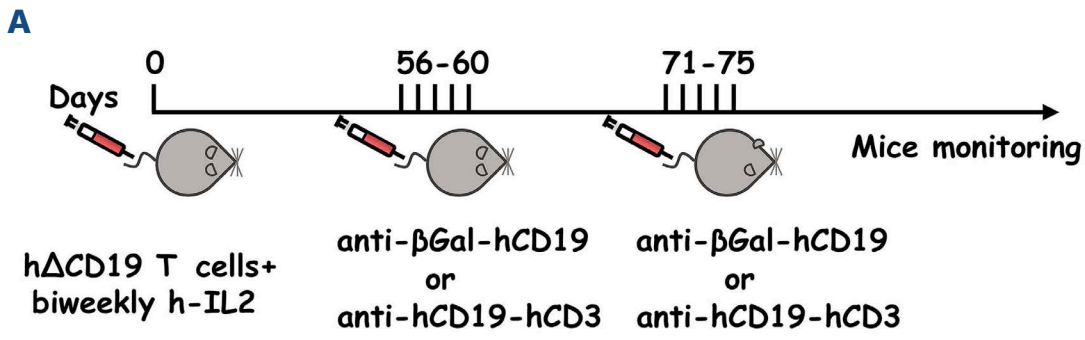

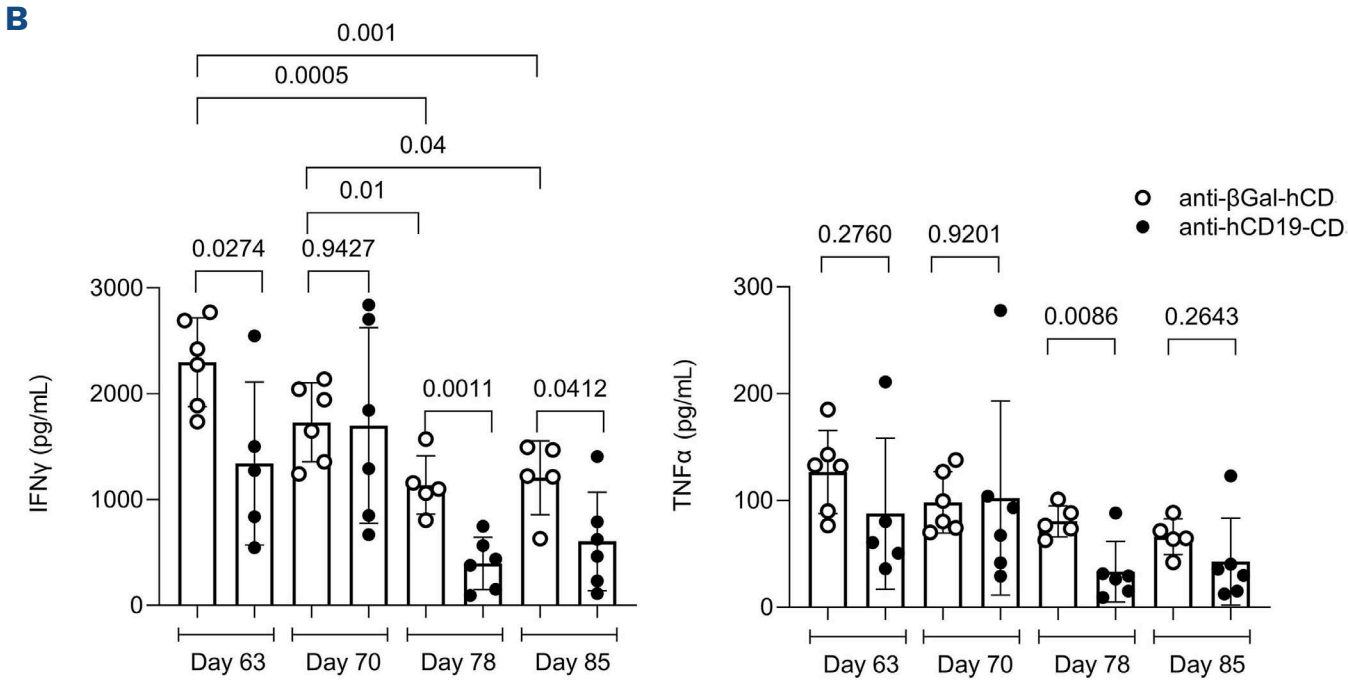

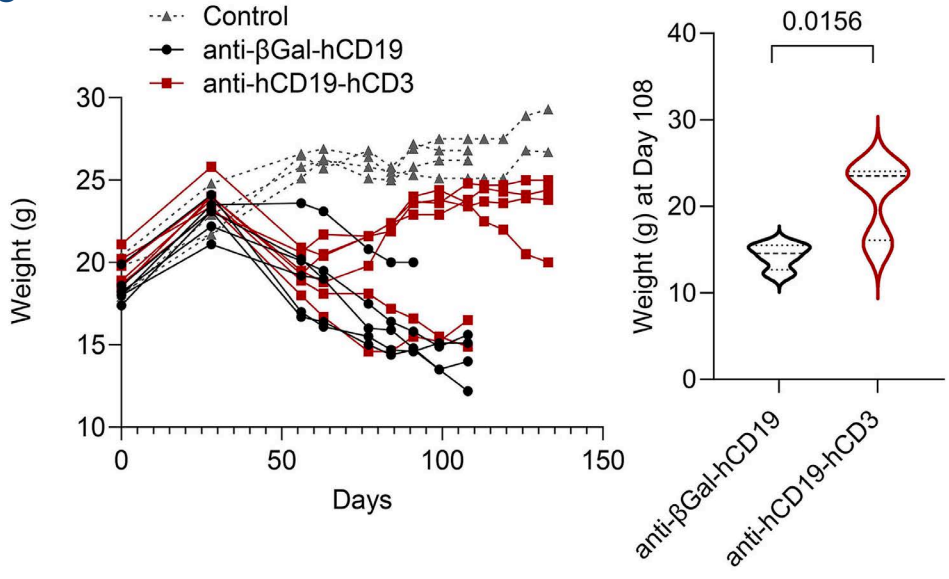

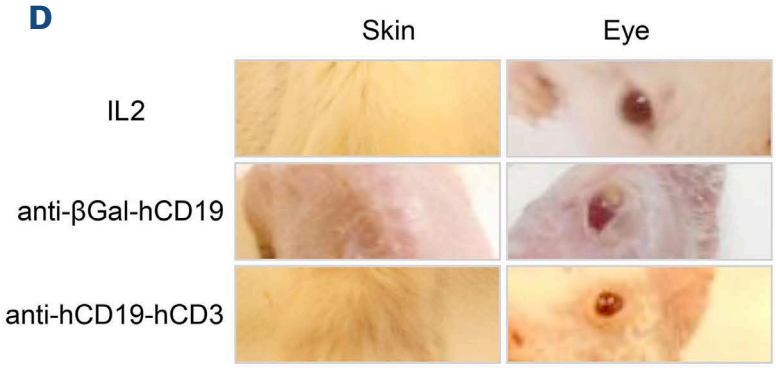

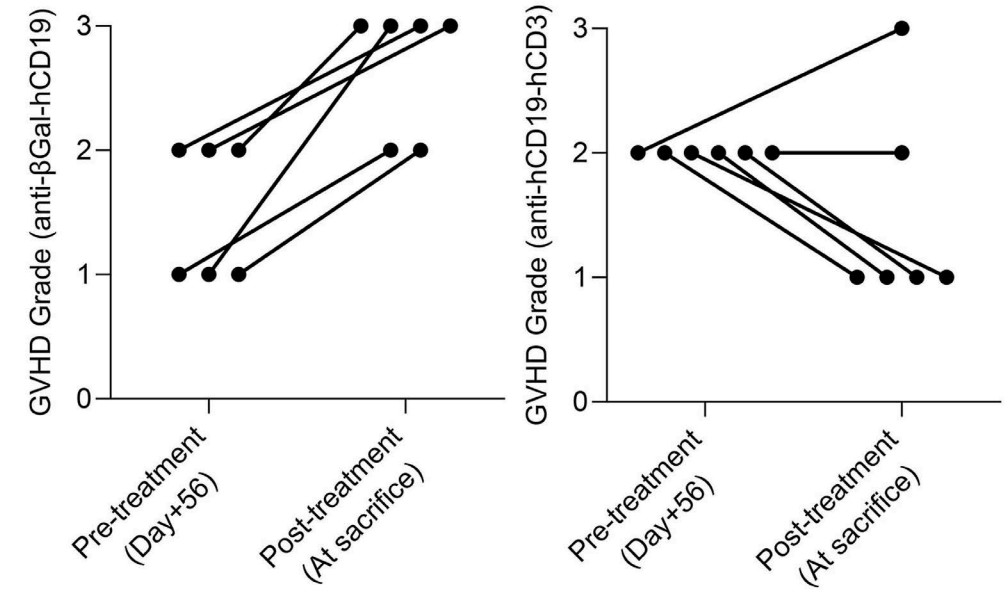

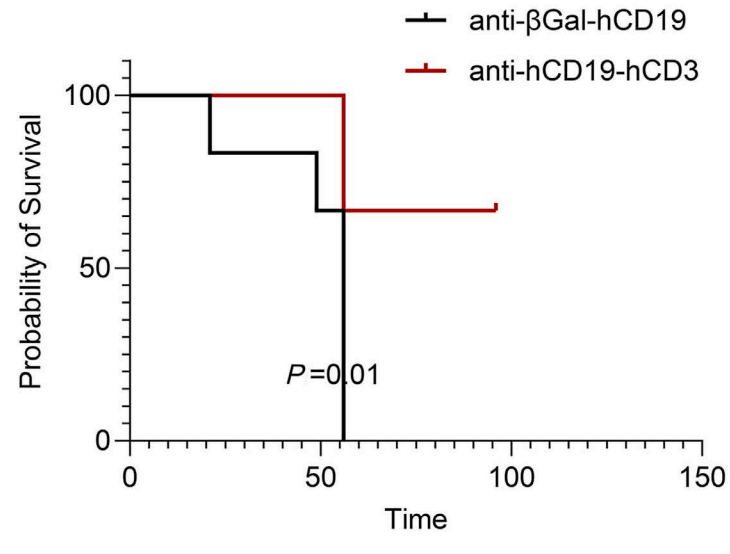

Continued on following page.

Figure 3. Anti-hCD19-hCD3 antibody displays a therapeutic effect in mice developing graft-*versus*-host disease. (A) Schematic representation of the *in vivo* experimental setting: mice developing graft-*versus*-host disease (GVHD) (N=12) were treated with either anti-βGal-hCD19 (N=6, 1 μg/mice/day) or anti-hCD19-hCD3 (N=6, 1 μg/mice/day) antibodies for 2 cycles of 5 days of drug administration. GVHD signs were monitored daily, while weight measurements and blood bleeding analysis were performed on a weekly basis. (B) IFNγ (left panel) and TNFα (right panel) levels were measured in peripheral blood of mice given either anti-βGal-hCD19 or anti-hCD19-hCD3 antibodies at day +63 and day +70 (corresponding to day 3 and 10 following the end of the first drug administration cycle) and at day +78 and day +85 (corresponding to day 3 and 10 following the end of the second drug administration cycle). Data are expressed as individual values ± standard deviation (SD). All data were compared by a two-tailed Student *t* test and *P* value <0.05 was considered to be statistically significant. (C) Left panel reports the weight monitoring during the entire study period of control mice (black dotted line), anti-βGal-hCD19-treated mice (black line) and anti-hCD19-hCD3-treated mice (red line). Right panel shows the weight measurement at day 108 (the last day of the animals undergoing the anti-βGal-hCD19 control treatment, which had to be sacrificed). (D) GVHD phenotypic manifestation in the interleukin 2 (IL2), anti-βGal-hCD19 and anti-hCD19-hCD3 treated mice. (E) Progression of GVHD severity at both the pre- and post-exposure to anti-βGal-hCD19 and anti-hCD19-hCD3 time points (F) Kaplan-Meier survival curve of hΔCD19 T-cell mice treated with either anti-βGal-hCD19 antibody (black line) or anti-hCD19-hCD3 antibody (red line).

panel) and the control cohort of anti-βGal-hCD19-treated (Figure 4C, bottom panel).

Notably, we did not observe any significant reduction in the mean of fluorescence intensity of CD19 expression in mice receiving anti-hCD19-CD3 at any time points compared to control mice (Figure 4D), suggesting that the BiTE targeting CD19 did not induce a selection of residual CD19$^+$ engineered T cells with a downregulation of CD19 expression. The different level of absolute number of hCD45$^+$ T cells in the two treatment cohorts of mice recorded overtime, are reported in Figure 4E, to clarify the statistically significant different absolute count of hCD45$^+$ T cells in the presence of the anti-hCD19-CD3 BiTE treatment with respect to controls.

Surviving mice of the cohort receiving the anti-hCD19-CD3 BiTE were euthanized (day 133) and organs commonly involved in GVHD pathophysiology were analyzed for the presence of human infiltrating T cells by the use of immunohistochemistry (IHC) (to assess CD3$^+$ T-cell tissue distribution) and immunofluorescence (to assess the proliferative state of the tissue-infiltrating CD3$^+$ T cells). Our study clearly shows that the percentage of tissue-infiltrating hCD45$^+$ T cells was significantly lower in the tissues of mice receiving anti-hCD19-CD3 BiTE compared to controls sacrificed for suffering at day 108 (Figure 5A, anti-CD3 IHC line), with the only exception of T-cell infiltrating the spleen. Moreover, the Ki67$^+$ staining was significantly higher in T cells infiltrating the skin and the spleen of control mice compared to that observed in mice treated with the anti-hCD19-CD3 BiTE (Figure 5A, B). The amount of hCD3$^+$ cells, as well as CD3$^+$ Ki67$^+$ cells, was quantified and presented in Figure 5B, showing a significant lower number of hCD3$^+$ or Ki67$^+$ T cells in tissues derived from mice treated with anti-hCD19-CD3 BiTE respect to controls.

Blinatumomab responder and non-responder mice have distinct circulating and tissue-resident T-cell subsets

We also performed a flow-cytometry analysis on T cells from murine peripheral blood or tissues to study the T-cell subset profile. First, we analyzed the distribution of CD4$^+$CD19$^+$ and CD8$^+$CD19$^+$ T-cell populations in the anti-hCD19-hCD3 and anti-βGal-hCD19 control cohorts (Figure 6). As shown in Figure 6A, C and E; and in *Online Supplementary Figure S3A*, *C* and *E*; CD4$^+$CD19$^+$ T cells accounted for the majority of T cells, being significantly higher compared to CD8$^+$CD19$^+$ T cells in all the tissues analyzed both in anti-hCD19-hCD3 and anti-βGal-hCD19-treated mice. Subsequently, we sought to investigate whether the treatment with anti-hCD19-hCD3 BiTE could impact the representation of memory cell subpopulations. By examining the dynamic states of T-cell differentiation, our findings indicate that in mice treated with anti-hCD19-hCD3 BiTE and with a significant improvement of GVHD manifestations (anti-hCD19-hCD3 responders), both CD4$^+$ and CD8$^+$ T cells show a significant higher percentage of central memory (CM) T cells in the peripheral blood, as compared with T cells found in the peripheral blood of control mice, in which the preponderant population was that of effector memory (EM) T cells (Figure 6B). Moreover, in both control mice and mice treated with anti-hCD19-hCD3 not improving GVHD manifestations (non-responders), T cells infiltrating liver and spleen were characterized by a terminal effector memory profile (TEMRA), whereas T cells infiltrating the same tissues in the responder mice were EM (Figure 6B, C).

Discussion

For many patients with hematological malignancies, allo-HSCT represents a valuable treatment option, whose efficacy is largely based on the GVL effect mediated, among others, by donor T lymphocytes. This T-cell mediated GVL effect can be further increased by the use of DLI. However, the therapeutic potential of DLI is limited by an increased GVHD risk, a serious complication associated with significant morbidity and mortality.[31]

The most extensively validated safety switch systems in clinical settings are the herpes-simplex thymidine kinase

(HSV-TK) and *iC9*. These suicide gene technologies can be broadly classified based on their mechanisms of action, which include either metabolic approaches (such as gene-directed enzyme prodrug therapy, or GDEPT) or dimerization-inducing strategies. HSV-TK is a well-known example of the GDEPT approach that, unlike the mam-

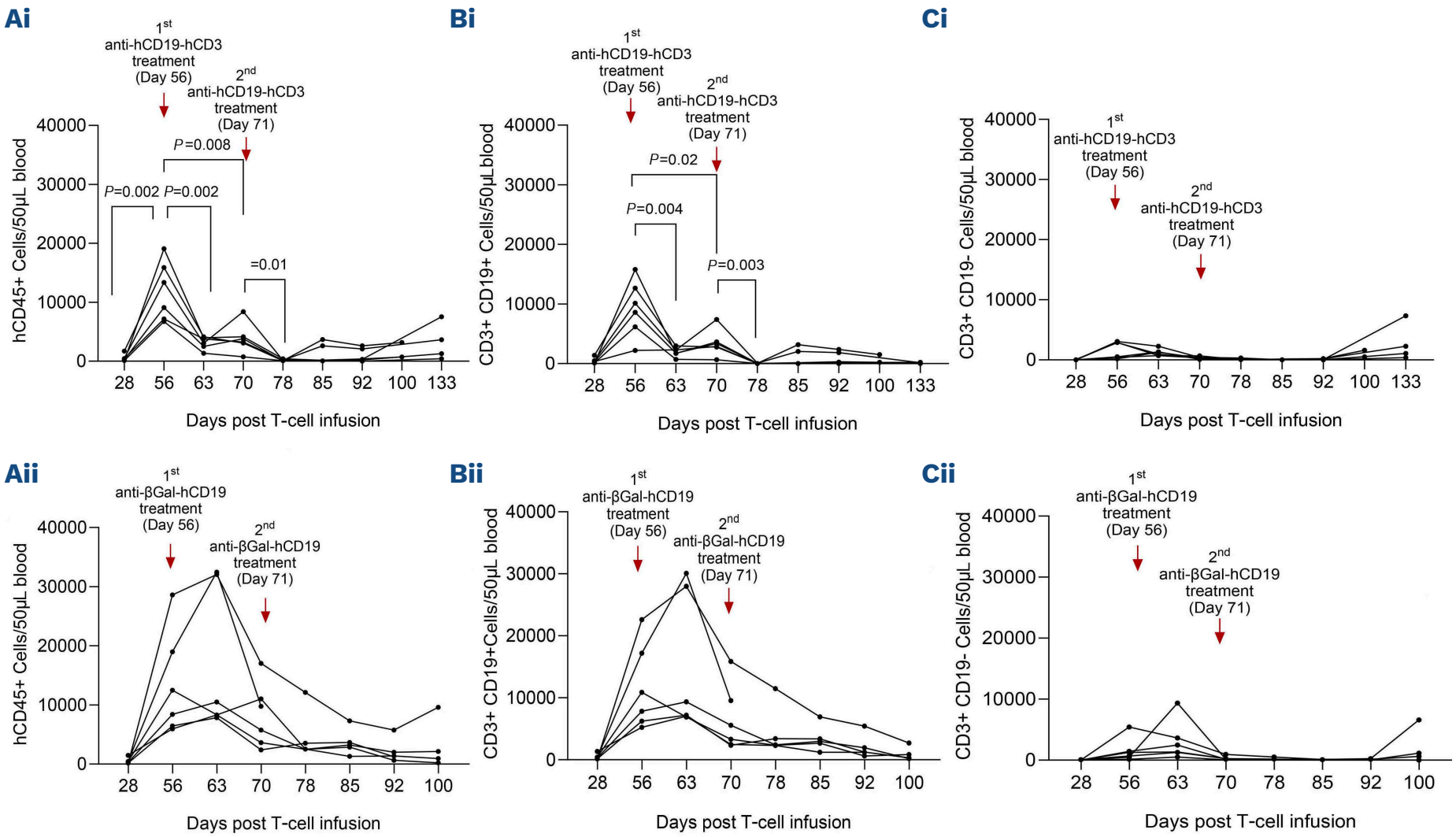

Figure 4. Anti-hCD19-hCD3 antibody eliminates hΔCD19 T cells in mice developing graft-*versus*-host disease. (A) Fluorescence-activated cell sorting (FACS) analysis was performed to evaluate the hCD45$^+$ cell distribution in peripheral blood of mice treated with either anti-hCD19-hCD3 (Ai) or anti-βGal-hCD19 (Aii) antibodies during the entire study period. Data are expressed as absolute cell count in 50 µL of blood, as individual values. (B) FACS analysis was performed to evaluate the CD3$^+$CD19$^+$ cell subset distribution in peripheral blood of mice treated with anti-hCD19-hCD3 (Bi) or anti-βGal-hCD19 (Bii) antibodies during the entire study period. Data are expressed as absolute cell count, as individual values. (C) FACS analysis was performed to evaluate the CD3$^+$CD19$^-$ cell subset distribution in peripheral blood of mice treated with anti-hCD19-hCD3 (Ci) and anti-βGal-hCD19 (Cii) antibodies during the entire study period. Data are expressed in absolute cell count, as individual values. (D) FACS analysis was performed to evaluate the CD19 mean fluorescence intensity (MFI) of hΔCD19 T cells in peripheral blood of mice treated with anti-βGal-hCD19 or anti-hCD19-hCD3 antibodies during the entire study period. Data are expressed in percentage, as individual values ± standard deviation (SD). (E) Statistical analysis of the data shown in Figure 4A to compare the 2 cohorts (mice treated with anti-βGal-hCD19 in Aii and anti-hCD19-hCD3 in (Ai) in order to highlight the statistical differences between these groups over time. Data are expressed as absolute cell count, as mean ± SD. All data were compared by a two-tailed Student *t* test and a *P* value <0.05 was considered to be statistically significant.

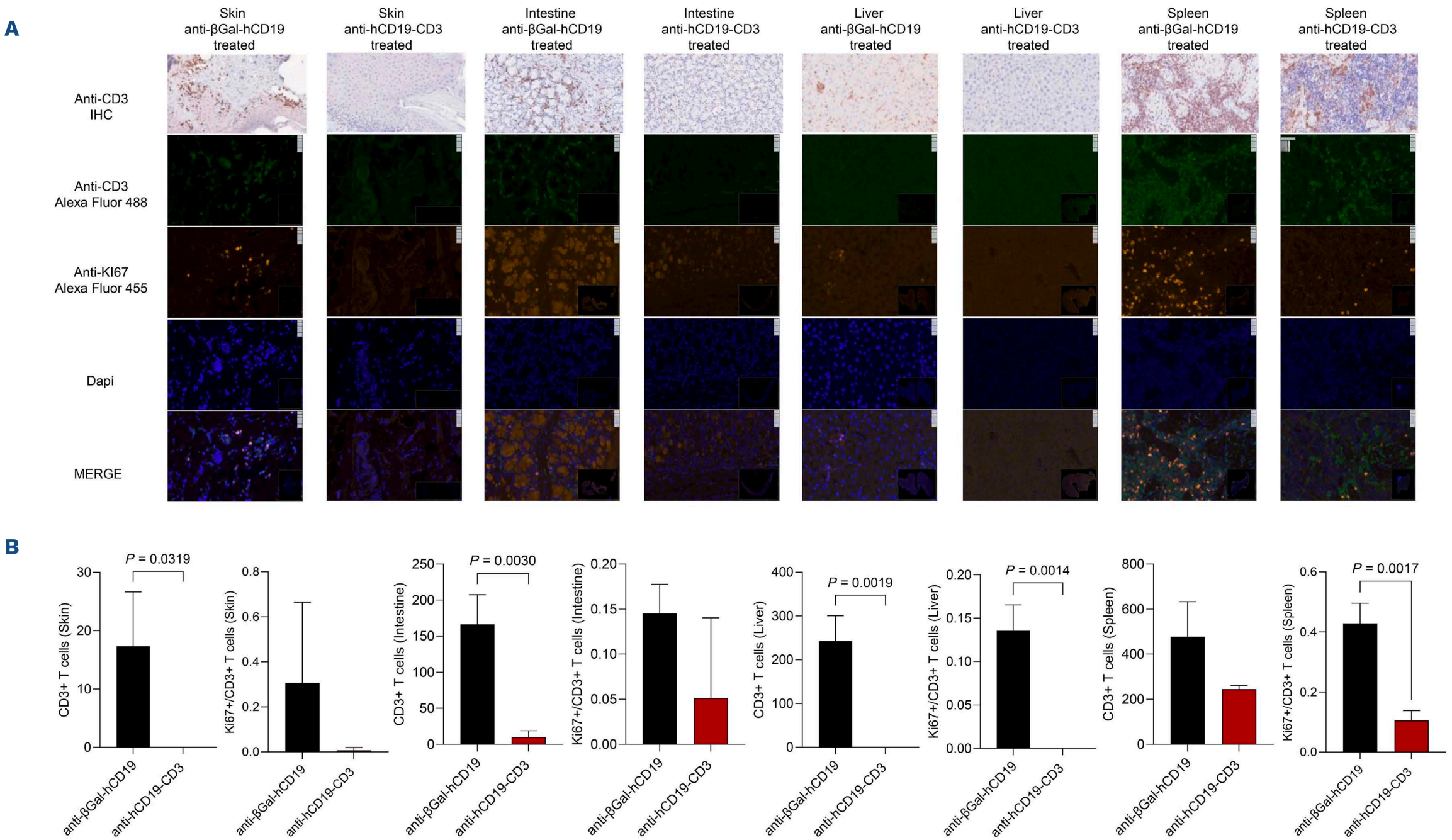

Figure 5. Anti-hCD19-hCD3 antibody modulates human cellular infiltrate in the tissues of mice developing graft-*versus*-host disease. (A) Anti-βGal-hCD19 and responding anti-hCD19-hCD3-treated mice were euthanized respectively at day +100 (due to mice suffering) and +133 (end of experiment), to perform immunohistochemistry (IHC) and immunofluorescence (IF) analysis on skin, intestine, liver and spleen evaluating the hCD3⁺ cell distribution (IHC first line, and IF in the second line) or Ki67⁺ cells (IF in the third line). The images were obtained under 40X magnification. (B) The amount of hCD3⁺ or Ki67⁺ cells was quantified using ImageJ software in three randomly selected areas of 0.4 mm² per slide and data were compared by a two-tailed Student *t* test; a *P* value <0.05 was considered to be statistically significant.

malian thymidine kinase, is characterized by 1,000-fold higher affinity to specific nucleoside analogues,[32] including ganciclovir (GCV), making it suitable for the use as a suicide gene in mammalian cells. Although it was shown that HSV-TK-modified T cells were able to persist in the circulation, and were sensitive to be eliminated effectively upon GCV administration,[33] immunogenicity remains a significant challenge, as the modified T cells can be recognized by the immune system and be destroyed. In addition, reduced immune function and impaired responses to viral infections can complicate its use, particularly in patients undergoing allo-HSCT.[34,34] By contrast, the *iC9* suicide gene is an example of apoptotic genes extensively used in clinical settings, especially for therapies involving genetically modified T cells, such as chimeric antigen receptor (CAR) T-cell therapies. It involves the expression of a modified form of caspase-9 which is engineered to be non-functional under normal conditions, but functional after administra-

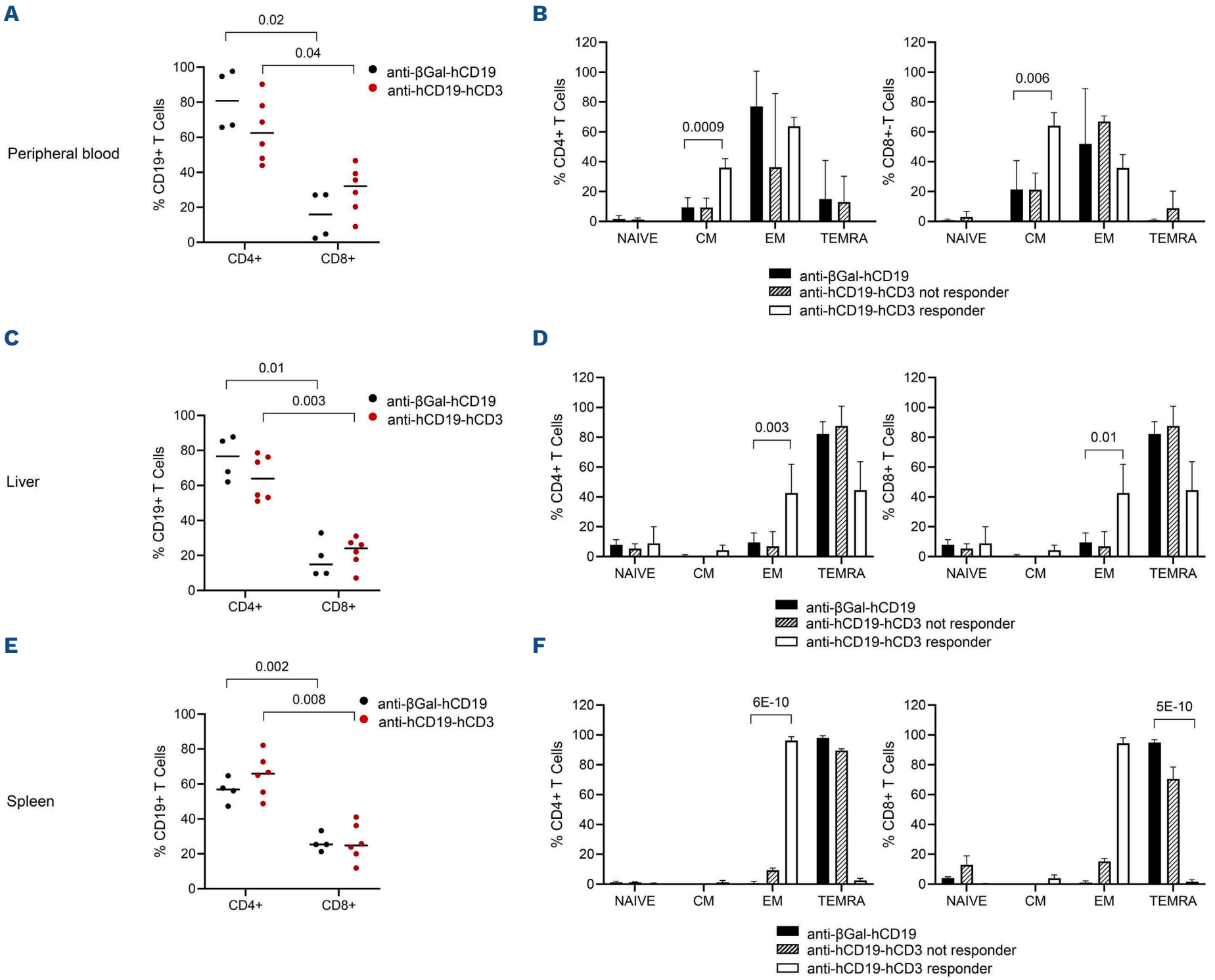

Figure 6. Anti-hCD19-hCD3 affects differently circulating and tissue-resident memory cells in responder and non-responder mice. Anti-βGal-hCD19 and responding anti-hCD19-hCD3-treated mice were euthanized respectively at day +100 (due to mice suffering) and +133 (end of experiment). Fluorescence-activated cell sorting (FACS) analysis was performed on peripheral blood (A), liver (C) and spleen (E) of both the control mice treated with anti-βGal-hCD19 and of those given the anti-hCD19-hCD3 to evaluate the $CD4^+CD19^+$ and $CD8^+CD19^+$ cell distribution. Data are expressed in percentage, as individual values. FACS analysis was performed to assess the T-cell subset profile in peripheral blood (B), liver (D) and spleen (F) in anti-βGal-hCD19 cohort and anti-hCD19-hCD3 responder or non-responder mice. In particular, for the definition of the memory T-cell subsets, the following analysis was applied: $CD4^+$ or CD8+ Naïve ($CD62L^+/CD45RA^+$), central memory (CM; $CD62L^+/CD45RA^-$), effector memory (EM, CD62L-/CD45RA-), terminal differentiated effector memory (TEMRA, $CD62L^-/CD45RA^+$). Data are expressed in percentage, as mean ± standard deviation. All data were compared by a two-tailed Student *t* test and a *P* value <0.05 was considered to be statistically significant.

tion of a small dimerizing molecule drug (such as AP1903 or AP20187), triggering the apoptotic pathway and leading to the selective elimination of the genetically modified T cells. Within 24 hours after exposure to the dimerizing molecule drug, this system offers near-complete T-cell[36] or CAR T-cell[27,37] depletion, making it highly effective in controlling T-cell persistence. Furthermore, compared to HSV-TK, the *iC9* system is characterized by a much lower immunogenicity, being *iC9* derived from a protein that is naturally present in human cells.[38,39] In this study, we investigated a novel monoclonal antibody-mediated safety switch mechanism using preclinical models designed to control the expansion of genetically modified T cells and thereby to manage GVHD manifestations. To this end, we engineered human T lymphocytes to express the extracellular domain of the CD19 antigen, generating $CD19^+CD3^+$ T cells. As *iC9*, the *ΔCD19* sequence is fully human, this minimizing its immunogenicity at difference with the HSV-TK strategy.[34] The genetic modification of T cells with ΔCD19 rendered the engineered T cell susceptible to the lytic action of an anti-hCD19-hCD3 BiTE molecule, which mimics the cytotoxic effect of blinatumomab - an Food and Drug Administration/European Medicines Agency-approved anti-hCD19-hCD3 bi-specific antibody used to target leukemia blasts in patients with B-cell precursor ALL.[24-26,40] In the event of GVHD, administration of the anti-hCD19-hCD3 BiTE can selectively eliminate $CD19^+CD3^+$ T lymphocytes through a fratricidal mechanism involving the mutual engagement of CD3 and CD19 antigens. The mechanism leading to the reduction of $CD19^+CD3^+$ T lymphocytes in culture after exposure to the BiTE was activated rapidly, with a significant decrease in transduced cells observed as early as 24 hours. This timing closely mirrors the effects seen with the *iC9* suicide gene system, but is notably faster than the apoptotic process triggered by ganciclovir exposure in HSV-TK cells.[41] We first confirmed the efficacy of anti-hCD19-hCD3 to selectively ablate ΔCD19-engineered T cells *in vitro* by studying hΔCD19 T cells in the presence of varying concentrations of the anti-hCD19-CD3 antibody. We observed a correlation between BiTE concentration and early kinetics of elimination of hΔCD19 T cells. Next, we developed an *in vivo* xenograft-reaction mouse model that mimics GVHD manifestations after engraftment of *ex vivo*-expanded, gene-modified human DLI represented by high numbers of hΔCD19 T cells. We assessed GVHD severity in mice using a scoring system, based on four distinct degrees of GVHD severity, which correlated with the percentage of expanded $hCD45^+$ cells, and the changes in inflammatory cytokine levels, notably IFNγ and TNFα. Although the model is not suitable for the evaluation of the GVL effect of ΔCD19-engineered T cells, it effectively recapitulates human GVHD pathology and provides a valuable platform for testing the therapeutic effects of the BiTE used in combination with hΔCD19 T cells. Indeed, this model allowed to develop GVHD signs in 75% of the mice by day 56. This timeline and frequency for GVHD onset are in the range of other more complex murine models of GVHD induced by the transplantation of T-cell-depleted bone marrow supplemented with varying numbers and phenotypic classes of donor lymphocytes (either splenocytes or lymph-node-derived T cells) into lethally irradiated recipients.[42] In these models, the bone marrow provides donor stem cells that allow hematopoietic reconstitution after irradiation (a key element of the model to induce tissue damage and cytokine storm), while T-cell depletion is carried out to control the dose and type of immune cells that are delivered. In our experimental setting, we sought to investigate a model of xeno-GVHD induced by *ex vivo* activated and gene-modified human T cells. In particular, several studies have shown that the CD3-induced cell activation required to transduce T cells and expand gene-modified cells leads to an impairment of alloreactivity in terms of GVHD induction and mortality,[43-46] compared with non-cultured, non-transduced resting T cells obtained from murine spleen cells or human PBMC. For these reasons, to develop an animal model in which to test the functionality of a novel suicide gene approach in the context of gene-modified T cells, we decided to infuse a large dose of hΔCD19 T cells in combination with recombinant human IL2. At the onset of GVHD symptoms, two cycles of anti-hCD19-CD3 BiTE were administered. Treatment with anti-hCD19-CD3 resulted in significant clinical improvements, including weight gain, reduction of fur loss and no abnormal eyeball growth compared to control animals. Importantly, we observed a marked reduction in GVHD severity in four of six animals and a statistically significant improvement in OS compared to control animals. The anti-hCD19-CD3 BiTE reduced significantly the circulating $hCD45^+$ cells, particularly $CD19^+$ $hCD3^+$ cells, which were sensitive to be further reduced by a second cycle of BiTE. Although not significant, we observed a slight re-expansion of the $CD19^+$ hT cells after the termination of the first BiTE cycle, suggesting that the antibody preferentially targeted xenoreactive T cells, while sparing less activated T cells. This observation is in line with previously published reports showing that, when iC9 was used as safety switch, the susceptibility to the AP1903 dimerizing drug was influenced by the activation status of the T cells, since the agent eliminated the most highly expressing and most highly transduced T cells, sparing quiescent gene-modified cells.[23] Previous studies have documented that transgene expression derived from retroviral constructs is highly dependent on the state of T-cell activation;[47] during GVHD, for example, alloreactive cells are the most activated, express the highest level of *iC9*, and therefore are the most readily eliminated after exposure to AP1903.[36] Moreover, we found that the re-expanded cells remained highly sensitive to the fratricidal mechanism triggered by a second challenge with the anti-hCD19-hCD3 BiTE. This finding is in line with a previously published report documenting the safety and efficiency of repeated activation of the iC9 safety switch for treatment for persistent or recurring toxicity from T-cell therapies.[21]

Further, our tissue analysis indicated that the reduction in GVHD manifestations was associated with decreased infiltration of $CD3^+$ T cells in GVHD target organs, contributing to the amelioration of disease symptoms and supporting the proposed mechanism of GVHD control via the targeted depletion of alloreactive T cells.

Lastly, the distinct profiles of memory T-cell subpopulations between responder and non-responder mice offer valuable insights into the immunological landscape following BiTE treatment. Responders exhibited a higher proportion of CM T cells, which are associated with long-term immune surveillance and potentially less inflammatory activity. By contrast, non-responder animals displayed a predominance of EM and TEMRA T cells, indicative of a more differentiated and potentially pro-inflammatory immune state. These findings suggest that successful GVHD management may involve not only the depletion of pathogenic T cells, but also the preservation or induction of a less differentiated and less inflammatory memory T-cell profile.

Our study provides compelling evidence that the infusion of hΔCD19 T cells, in combination with the anti-hCD19-hCD3 BiTE, represents a promising therapeutic approach to accelerate the restoration of adaptive immunity, while offering an effective control of GVHD manifestations in case this complication occurs. In addition, in the context of B-cell malignancies, the administration of anti-hCD19-hCD3 BiTE may help not only to control toxicity of $CD3^+CD19^+$ cells, but also to eventually target re-emerging leukemic B cells, potentially enhancing the overall GVL effect and strengthening the antitumor response. The transient depletion of peripheral B cells following the infusion of an anti-hCD19-hCD3 BiTE to control GVHD after DLI is unlikely to markedly impact the reconstitution of B-cell precursors of HSCT recipients. This is due to the drug's short half-life and the brief duration of anti-hCD19-hCD3 BiTE infusion required to induce apoptosis in allo-reactive $CD19^+$ T cells, in contrast to the continuous 28-day i.v. infusion regimen used in BCP-ALL patients.[48] Likewise, B-cell recovery after HSCT is not expected to sequester anti-hCD19-hCD3 to an extent that would prevent effective depletion of $CD19^+$ $CD3^+$ cells. The approach we have developed can be also used as a safety switch in CAR T-cell constructs, other than those targeting CD19, such as constructs targeting GD2 or CD7 antigens.[49,50] The selective/preferential targeting of alloreactive T cells while sparing non-alloreactive ones offers a novel and potentially safer method to mitigate the adverse effects associated with DLI in allo-HSCT recipients. Future clinical studies are warranted to validate these preclinical findings and optimize the dosing and administration strategies of the BiTE to maximize therapeutic efficacy, while minimizing potential drawbacks.

Disclosures

GZ is employed by Amgen and holds stock. GZ reports issue of patents (20190300609, 20130323247, and 20110262440), and has patents pending (10696744, 10662243, 20190142846, 20190142846, 20170327581, 10130638, 9688760, 20170122947, 9486475, 20160208001, 9192665, 20150071928, 8840888, 20140228316, 20140227272, 20130287778, and 20130287774). All other authors have no conflicts of interest to disclose.

Contributions

CQ, BDA, SM and FL designed the experimental studies and supervised the project conduction. SM, CQ, BDA and FL analyzed the data and wrote the manuscript. SM, LI, MG and RDV developed the in vitro models and performed the in vitro experiments. SM, CQ, BDA, LI, MG, and RDV performed the in vivo experiments. PM, FDB, MB, MA, DP, GZ and FL provided their expertise to define the clinical translation perspective. BDA, SM, CQ, GZ and FL revised the final version of the manuscript. All authors read and approved the final manuscript.

Acknowledgments

We are very grateful to BioVec Pharma and Dr Manuel Caruso in providing the packaging cell line 293Vec-RD114 used for the generation of the retroviral vector used for the manufacturing of ΔCD19-engineered T cells. We are very grateful to OPBG Cytometry (in particular, Dr Ezio Giorda, Dr Marco Scarsella and Gabriele Volpe) and Pathology (in particular, Dr Marco Pezzullo and Dr Cristiano De Stefanis) Facilities for supporting our in vitro experiments. We are very grateful to patients associations that support our research: Associazione "Un...due...tre...Alessio" (to FL); Famiglia Lazzari (to CQ); Associazione "Passarelli" (to BDA).

Funding

The experimental work was supported by grants awarded by (i) the Associazione Italiana Ricerca per la Ricerca sul Cancro (investigator grant AIRC-IG ID. 29057) (to BDA); MFAG 25106 (to CQ); Special Project 5×1000 no. 9962 (to FL); (ii) the Italian Ministry of Health: Ricerca Corrente 5X1000 (to BDA and SM); Ricerca Finalizzata RF-2021-12374120 (to CQ); Progetto Ministeriale CAR T (to FL); PNC LSH-TA Ecosistema innovativo della Salute (F. Locatelli); PNRR rare tumors PNRR-TR1-2023-12378404 (to BDA); (iii) the Italian Ministry of University and Research; Italian PNRR CN3 "National Center for Gene Therapy and Drugs based on RNA Technology" (to FL); PRIN 2020 (to FL), PRIN 2022 (to FL and CQ); (iv) Ministero delle Imprese e del Made in Italy (MISE); POS project Life Science Hub Regione Puglia (to FL); F/260019/01/04/X51 (to CQ); "PatENts in tHe medicAl aNd for CompaniEs - ENHANCE" (to BDA). Ministero dello sviluppo Economico: Bando 2023 Filiere produttive (to FL); IMI JU/T2EVOLVE grant no. 945393 (to FL).

Data-sharing statement

The authors confirm that the data supporting the findings of this study are available upon specific request to the corresponding authors.

References

1. Saadeh SS, Litzow MR. Hematopoietic stem cell transplant in adults with acute lymphoblastic leukemia: the present state. Expert Rev Hematol. 2018;11(3):195-207.
2. Copelan EA. Hematopoietic stem-cell transplantation. N Engl J Med. 2006;354(17):1813-1826.
3. Fuchs KJ, Falkenburg JHF, Griffioen M. Minor histocompatibility antigens to predict, monitor or manipulate GvL and GvHD after allogeneic hematopoietic cell transplantation. Best Pract Res Clin Haematol. 2024;37(2):101555.
4. D'Souza A, Fretham C, Lee SJ, et al. Current use of and trends in hematopoietic cell transplantation in the United States. Biol Blood Marrow Transplant. 2020;26(8):e177-e182.
5. Frey NV, Porter DL. Graft-versus-host disease after donor leukocyte infusions: presentation and management. Best Pract Res Clin Haematol. 2008;21(2):205-222.
6. Porter DL, Levine BL, Bunin N, et al. A phase 1 trial of donor lymphocyte infusions expanded and activated ex vivo via CD3/CD28 costimulation. Blood. 2006;107(4):1325-1331.
7. Malard F, Holler E, Sandmaier BM, Huang H, Mothy M. Acute graft-versus-host disease. Nat Rev Dis Primers. 2023;9(1):27.
8. Ghimire S, Weber D, Mavin E, et al. Pathophysiology of GvHD and other HSCT-related major complications. Front Immunol. 2017;8:79.
9. Jamil MO, Mineishi S. State-of-the-art acute and chronic GVHD treatment. Int J Hematol. 2015;101(5):452-466.
10. Ferrara JL, Levine JE, Reddy P, Holler E. Graft-versus-host disease. Lancet. 2009;373(9674):1550-1561.
11. Blazar BR, Hill GR, Murphy WJ. Dissecting the biology of allogeneic HSCT to enhance the GvT effect whilst minimizing GvHD. Nat Rev Clin Oncol. 2020;17(8):475-492.
12. Collins RH, Jr., Shpilberg O, Drobyski WR, et al. Donor leukocyte infusions in 140 patients with relapsed malignancy after allogeneic bone marrow transplantation. J Clin Oncol. 1997;15(2):433-444.
13. Urbano-Ispizua A, Brunet S, Solano C, et al. Allogeneic transplantation of CD34+-selected cells from peripheral blood in patients with myeloid malignancies in early phase: a case control comparison with unmodified peripheral blood transplantation. Bone Marrow Transplant. 2001;28(4):349-354.
14. Roldan E, Perales MA, Barba P. Allogeneic stem cell transplantation with CD34+ cell selection. Clin Hematol Int. 2019;1(3):154-160.
15. Ho VT, Soiffer RJ. The history and future of T-cell depletion as graft-versus-host disease prophylaxis for allogeneic hematopoietic stem cell transplantation. Blood. 2001;98(12):3192-3204.
16. Handgretinger R. New approaches to graft engineering for haploidentical bone marrow transplantation. Semin Oncol. 2012;39(6):664-673.
17. Li Pira G, Malaspina D, Girolami E, et al. Selective depletion of alphabeta T cells and B cells for human leukocyte antigen-haploidentical hematopoietic stem cell transplantation. A three-year follow-up of procedure efficiency. Biol Blood Marrow Transplant. 2016;22(11):2056-2064.
18. Locatelli F, Merli P, Pagliara D, et al. Outcome of children with acute leukemia given HLA-haploidentical HSCT after alphabeta T-cell and B-cell depletion. Blood. 2017;130(5):677-685.
19. Merli P, Algeri M, Galaverna F, et al. TCRalphabeta/CD19 cell-depleted HLA-haploidentical transplantation to treat pediatric acute leukemia: updated final analysis. Blood. 2024;143(3):279-289.
20. Pietro Merli VB, Federica Galaverna, Mattia Algeri, et al. Donor T cells genetically modified with a novel suicide gene (inducible caspase 9, iC9) expand and persist over time after post-allograft infusion in patients given αβ T-cell and B-cell depleted HLA-haploidentical allogeneic stem cell transplantation (αβ haplo-HSCT) contributing to accelerate immune recovery. Blood. 2017;130(Suppl 1):211.
21. Zhou X, Naik S, Dakhova O, Dotti G, Heslop HE, Brenner MK. Serial activation of the inducible caspase 9 safety switch after human stem cell transplantation. Mol Ther. 2016;24(4):823-831.
22. Zhou X, Dotti G, Krance RA, et al. Inducible caspase-9 suicide gene controls adverse effects from alloreplete T cells after haploidentical stem cell transplantation. Blood. 2015;125(26):4103-4113.
23. Tey SK, Dotti G, Rooney CM, Heslop HE, Brenner MK. Inducible caspase 9 suicide gene to improve the safety of allodepleted T cells after haploidentical stem cell transplantation. Biol Blood Marrow Transplant. 2007;13(8):913-924.
24. von Stackelberg A, Locatelli F, Zugmaier G, et al. Phase I/phase II study of blinatumomab in pediatric patients with relapsed/refractory acute lymphoblastic leukemia. J Clin Oncol. 2016;34(36):4381-4389.
25. Gokbuget N, Dombret H, Bonifacio M, et al. Blinatumomab for minimal residual disease in adults with B-cell precursor acute lymphoblastic leukemia. Blood. 2018;131(14):1522-1531.
26. Brown PA, Ji L, Xu X, et al. Effect of postreinduction therapy consolidation with blinatumomab vs chemotherapy on disease-free survival in children, adolescents, and young adults with first relapse of B-cell acute lymphoblastic leukemia: a randomized clinical trial. JAMA. 2021;325(9):833-842.
27. Guercio M, Manni S, Boffa I, et al. Inclusion of the inducible caspase 9 suicide gene in CAR construct increases safety of CAR CD19 T cell therapy in B-cell malignancies. Front Immunol. 2021;12:755639.
28. Orlando D, Miele E, De Angelis B , et al. Adoptive immunotherapy using PRAME-specific T cells in medulloblastoma. Cancer Res. 2018;78(12):3337-3349.
29. Ciccone R, Quintarelli C, Camera A, et al. GD2-targeting CAR T-cell therapy for patients with GD2+ medulloblastoma. Clin Cancer Res. 2024;30(11):2545-2557.
30. Choi J, Cooper ML, Staser K, et al. Baricitinib-induced blockade of interferon gamma receptor and interleukin-6 receptor for the prevention and treatment of graft-versus-host disease. Leukemia. 2018;32(11):2483-2494.
31. Zeiser R, Blazar BR. Acute graft-versus-host disease. N Engl J Med. 2018;378(6):586.
32. Elion GB, Furman PA, Fyfe JA, de Miranda P, Beauchamp L, Schaeffer HJ. Selectivity of action of an antiherpetic agent, 9-(2-hydroxyethoxymethyl) guanine. Proc Natl Acad Sci U S A. 1977;74(12):5716-5720.
33. Greco R, Oliveira G, Stanghellini MT, et al. Improving the safety of cell therapy with the TK-suicide gene. Front Pharmacol. 2015;6:95.
34. Berger C, Flowers ME, Warren EH, Riddel SR. Analysis of transgene-specific immune responses that limit the in vivo persistence of adoptively transferred HSV-TK-modified donor T cells after allogeneic hematopoietic cell transplantation. Blood. 2006;107(6):2294-2302.
35. Sauce D, Bodinier M, Garin M, et al. Retrovirus-mediated gene transfer in primary T lymphocytes impairs their anti-Epstein-

Barr virus potential through both culture-dependent and selection process-dependent mechanisms. Blood. 2002;99(4):1165-1173.
36. Straathof KC, Pule MA, Yotnda P, et al. An inducible caspase 9 safety switch for T-cell therapy. Blood. 2005;105(11):4247-4254.
37. Quintarelli C, Orlando D, Boffa I, et al. Choice of costimulatory domains and of cytokines determines CAR T-cell activity in neuroblastoma. Oncoimmunology. 2018;7(6):e1433518.
38. Di Stasi A, Tey SK, Dotti G, et al. Inducible apoptosis as a safety switch for adoptive cell therapy. N Engl J Med. 2011;365(18):1673-1683.
39. Gargett T, Brown MP. The inducible caspase-9 suicide gene system as a "safety switch" to limit on-target, off-tumor toxicities of chimeric antigen receptor T cells. Front Pharmacol. 2014;5:235.
40. Locatelli F, Zugmaier G, Rizzari C, et al. Effect of blinatumomab vs chemotherapy on event-free survival among children with high-risk first-relapse B-cell acute lymphoblastic leukemia: a randomized clinical trial. JAMA. 2021;325(9):843-854.
41. Tiberghien P, Ferrand C, Lioure B, et al. Administration of herpes simplex-thymidine kinase-expressing donor T cells with a T-cell-depleted allogeneic marrow graft. Blood. 2001;97(1):63-72.
42. Schroeder MA, DiPersio JF. Mouse models of graft-versus-host disease: advances and limitations. Dis Model Mech. 2011;4(3):318-333.
43. Mercier-Letondal P, Montcuquet N, Sauce D, et al. Alloreactivity of ex vivo-expanded T cells is correlated with expansion and CD4/CD8 ratio. Cytotherapy. 2008;10(3):275-288.
44. Contassot E, Murphy W, Angonin R, et al. In vivo alloreactive potential of ex vivo-expanded primary T lymphocytes. Transplantation. 1998;65(10):1365-1370.
45. Weijtens M, van Spronsen A, Hagenbeek A, Braakman E, Martens A. Reduced graft-versus-host disease-inducing capacity of T cells after activation, culturing, and magnetic cell sorting selection in an allogeneic bone marrow transplantation model in rats. Hum Gene Ther. 2002;13(2):187-198.
46. Drobyski WR, Majewski D, Ozker K, Hanson G. Ex vivo anti-CD3 antibody-activated donor T cells have a reduced ability to cause lethal murine graft-versus-host disease but retain their ability to facilitate alloengraftment. J Immunol. 1998;161(5):2610-2619.
47. Quinn ER, Lum LG, Trevor KT. T cell activation modulates retrovirus-mediated gene expression. Hum Gene Ther. 1998;9(10):1457-1467.
48. Przepiorka D, Ko CW, Deisseroth A, et al. FDA approval: blinatumomab. Clin Cancer Res. 2015;21(18):4035-4039.
49. Del Bufalo F, De Angelis B, Caruana I, et al. GD2-CART01 for relapsed or refractory high-risk neuroblastoma. N Engl J Med. 2023;388(14):1284-1295.
50. Png YT, Vinanica N, Kamiya T, Shimasaki N, Coustan-Smith E, Campana D. Blockade of CD7 expression in T cells for effective chimeric antigen receptor targeting of T-cell malignancies. Blood Adv. 2017;1(25):2348-2360.